

P7.10 SIMULTANEOUS REMOTE SENSING OF THIN CIRRUS AND AEROSOL PROPERTIES FROM MODIS DATA

J. K. Roskovensky* and K. N. Liou

Department of Atmospheric and Oceanic Sciences, University of California, Los Angeles, California, USA

1. INTRODUCTION

Tropospheric aerosols and thin cirrus clouds play an important role in the atmospheric radiation budget. The occurrence of both appears ubiquitous and, while it would be valuable to obtain their microphysical properties simultaneously, distinguishing between the two optically thin media from space is extremely difficult. Presently, retrieval of aerosol and cirrus properties by satellites are made separately, but there is evidence that thin/sub-visible cirrus may be substantially more widespread than is currently being detected (Wylie and Menzel, 1999), especially in the tropics (Dessler and Yang, 2003), and is leading to large errors in the retrieved aerosol properties (Mishchenko et al., 1999). We present a procedure to retrieve thin cirrus and aerosol optical depth, as well as cirrus ice crystal effective size, over the ocean using MODIS bands 1, 2, 6, and 26 when they occur in the same field-of-view. Surface reflectance, the leading source of error, is quantified from observed clear sky reflectance for appropriate viewing geometry. We validate our results using both mm-wave radar data and AERONET aerosol optical retrievals from the Tropical Western Pacific-Atmospheric Radiation Measurement (TWP-ARM) site located on the island Republic of Nauru. Operational MODIS retrievals are also examined for comparison purposes. We believe that this new method can increase the total area in which aerosol information is obtained while reducing the effect that thin cirrus contamination has upon the aerosol retrieval.

2. RETRIEVAL METHOD

Cirrus clouds are generally located above most tropospheric aerosols. For visible reflectance with wavelength greater than 0.64 μm , the effects of molecular scattering is relatively weaker than that due to clouds and aerosols particles, and the apparent reflection at the top of the atmosphere can be approximated by the sum of the three terms identified with cirrus reflectance (r_c), aerosol reflectance (r_a), and the surface reflectance (r_s) as follows:

$$r = r_c + t_c \cdot r_a \cdot t_c^* + t_c \cdot t_a \cdot r_s \cdot t_a^* \cdot t_c^* \quad (1)$$

where t_c and t_a represent the cirrus and aerosol

transmittance, respectively, and * denotes the upwelling contribution. The reflectance due to aerosols can then be estimated by

$$r_a = \frac{r - r_c' + (1 - t_c'') \cdot r_{clr}}{t_c''} \quad (2)$$

where the clear column reflectance, r_{clr} , the apparent cirrus reflectance, r_c' , and the two-way cirrus transmittance, t_c'' , are defined by the following expressions:

$$r_{clr} = t_a \cdot r_s \cdot t_a^* \quad (3a)$$

$$r_c' = r_c + r_{clr} \quad (3b)$$

$$t_c'' = t_c \cdot t_c^* \quad (3c)$$

The cirrus transmittances are estimated by $1 - r_c$. The parameterized equation denoted in Eq. (1) has been verified by using an exact adding-method radiative transfer calculation where TOA reflectances are within 0.1% for small aerosol and cirrus optical depths (<0.5).

In order to accurately estimate the aerosol reflectance, both the reflectance due to cirrus only and the reflectance off the surface must be determined with precision. In the present study, the surface reflectance was obtained by averaging a large amount of neighboring observed clear sky pixels that were determined by five tests. The first test used was the standard visible reflectance test for ocean surface taken directly from the MODIS cloud mask (Ackerman et al., 2002). The next two tests examined spatial uniformity and required a 5x5 group of pixels to have 0.65 μm standard deviation below 0.25% following Martins et al. (2002) and 11 μm BT standard deviation less than 0.5 K. The last two, the 8.6 – 11 μm brightness temperature difference test and the 1.87 $\mu\text{m}/0.65 \mu\text{m}$ reflectance ratio test, specifically target thin cirrus, as described in Roskovensky and Liou (2003). Since any of the tests could prohibit pixels from being classified as clear, this procedure is clear sky conservative. To obtain the best estimate of true surface reflectance without an aerosol contribution, we subtract one standard deviation from the mean clear sky value with the understanding that aerosols contribute more significantly to the variance in the measurements.

Cirrus reflectance in a visible band between 0.4-1.0 μm , $r_{c,vis}$, is correlated to cirrus reflectance in the 1.38 μm band, $r_{c,138}$, (Gao and Kaufman, 1995) by

$$r_{c,138} = c^* r_{c,vis} + d \quad (4)$$

* Corresponding author address: John K. Roskovensky, Univ. of California, Los Angeles, Box 951565, Los Angeles, CA 90095, e-mail: jrosko@atmos.ucla.edu.

where c is the correlation between the two bands and d depends on the absorption, scattering and reflection below the cirrus cloud level both given as a function of viewing geometry. We find the value of c as the slope of a best-fit line through 100 visible reflectance points correlated with $1.38\ \mu\text{m}$ reflectance defined by 100 bins in the range between 0-10% with 0.1% resolution. These points were determined from the mean of the cluster of minimum visible reflectance values in each $1.38\ \mu\text{m}$ reflectance bin when examining observed cirrus reflectance. By using the observed surface reflectance as a measure of d , the observed $1.38\ \mu\text{m}$ reflectance, and c , cirrus reflectance in the $0.65\ \mu\text{m}$ and $0.86\ \mu\text{m}$ channels can be determined. An example of this procedure from a case study is shown in Fig. 1. The scatter of $0.65\ \mu\text{m}$ versus $1.38\ \mu\text{m}$ reflectance is presented for all points in a defined scattering angle from one MODIS granule. The left most line, barely visible through the dense cluster of points, represents the cirrus reflectance correlation line. The small vertical part connects the x-axis with the observed surface reflectance point. The residual term representing below cirrus reflectance is found by subtracting the calculated cirrus reflectance from the observed reflectance as a function of $1.38\ \mu\text{m}$ reflectance which can be seen as the horizontal difference between the points and the cirrus reflectance correlation line in Fig. 1. This term is only found for points between the cirrus reflectance correlation line and a maximum aerosol reflectance line correlating to an aerosol optical depth just over 0.5 shown as the right line in Fig. 1. Any points to the right of that line potentially result from low clouds that produce higher visible reflectance. Also, no retrievals were made on pixels if their $1.38\ \mu\text{m}$ reflectance was over 10%.

Aerosol optical depths (AOD) were retrieved by matching the residual term, adjusted for cirrus transmittance as in Eq. (2), in the $0.65\ \mu\text{m}$ and $0.86\ \mu\text{m}$ bands to 1-D look-up tables (LUT) that were produced using correct viewing geometry and retrieved surface reflectance. The average of the two values correlated to $0.55\ \mu\text{m}$ was used as the final AOD value. The LUT reflectances were calculated for a sequence of 11 aerosol optical depths from 0.0 to 0.5 using the adding/doubling method in the radiative transfer model described in Takano and Liou (1989) for different aerosol optical depths. Aerosol single-scattering properties were those of a clean-maritime distribution taken from D'Almeida et al. (1991). To maintain a high signal-to-noise ratio, analysis was performed on a group of 25 MODIS pixels defined as 5 pixels in 5 adjacent scan lines. This resulted in a retrieval resolution of $5\ \text{km} \times 5\ \text{km}$ at nadir. The cirrus optical depth (COD) and effective ice crystal size were then retrieved on a $1\ \text{km}$ pixel resolution using observed reflectance in each of the $0.65\ \mu\text{m}$ and $0.86\ \mu\text{m}$ bands paired with the $1.64\ \mu\text{m}$ reflectance and finding the best fit among pre-calculated

reflectances of a 2-D LUT, correlated to the retrieved aerosol optical depth, surface reflectance, and viewing geometry. This table was constructed by the same radiative transfer program but employed nonspherical ice-crystal single-scattering properties that included seven ice crystal size distributions composed of 50% bullet rosettes, 30% hollow columns, and 20% solid plates described in Heymsfield and Platt (1984), Takano and Liou (1989), and Liou (2002) with effective size ranging from $10\text{--}124\ \mu\text{m}$, as defined in Eq. (3) in Rolland et al. (2000). This procedure is similar to that performed operational on MODIS data (King et al., 1997), except that the LUT had much finer optical depth resolution (0.1) so that bilinear interpolation could be used. Based on an 8% surface reflectance error, or the average surface reflectance standard deviation, uncertainties in AOD ranged from 41% to 23% as the AOD increased from 0.1 to 0.2. Uncertainties in COD result from combined errors in surface reflectance and AOD and are estimated to be 48% and 9% when the COD is 0.1 and 0.5, respectively. Errors in the effective ice crystal size can be large when cirrus is very thin.

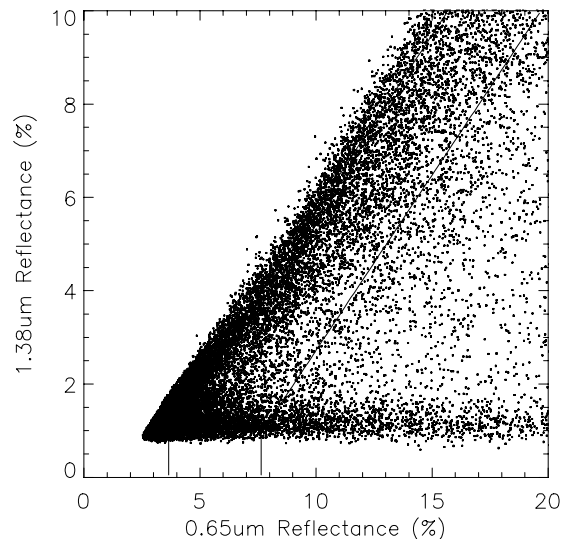


Figure 1. Scatter plot of all points defined with satellite scan angle between 0° and 5° from the MODIS granule on September 22, 2001 (2330 UTC). The two lines indicate the cirrus reflectance and the aerosol/low cloud cut-off from left to right, respectively.

3. CASE STUDIES: DATA AND VALIDATION

Radiometric data was obtained from the MODIS instrument onboard the Terra satellite. Three specific cases in 2001 [September 13 (2330 UTC), September 22 (2325 UTC), and October 4 (2350 UTC)] were chosen over the TWP-ARM site ($0.32^\circ\ \text{S}$, $166.55^\circ\ \text{E}$) where mm-wave radar indicated the presence of thin cirrus without a great deal of low cloud and, at the same

time, AERONET aerosol optical depth retrievals were available. In each case, at least 3 three AERONET AOD data points (AERONET AOD are calculated every 15 minutes) were available within the 3-hour period when MODIS flew over in these cases. MODIS data was analysis from a 51 x 51 pixel region centered on the TWP-ARM Nauru site. The approximate 50 km size was chosen since it engulfed the cirrus seen in a 1-hour cloud radar time series and a 3-hour AERONET time series as calculated by cirrus and aerosol level winds. Unfortunately, on September 13 (S13), this region was in strong sun glint. On September 22 (S22) the region was located near the sun glint border where reflection was weakly enhanced. The October 4 (O4) had no sun glint influence.

Table 1. AOD and COD comparisons for 3 TWP-ARM cases.

Method	9-13 2001		9-22 2001		10-4 2001	
	AOD	COD	AOD	COD	AOD	COD
Retrievals ^a	0.21	1.56	0.142	0.20	0.22	0.44
MODIS ^b	N/A	1.44	N/A	2.55	N/A	1.07
Radar ^c	N/A	0.46-0.91	N/A	0.2-0.3	N/A	0.1-0.61
AERONET ^d	0.16-0.3	N/A	0.12-0.15	N/A	0.17-0.3	N/A

^aMean retrieved values. ^bMean MODIS products. ^cCOD range calculated from the 1-hour mm-wave radar cloud thickness time series. ^dAOD range from the 3-hour AERONET time series.

Table 1 displays the comparisons between the retrieved mean property values, the mean operational MODIS retrievals, the range of COD values determined by the product of the 1-hour mm-wave radar cloud thickness time series and the theoretical cirrus extinction coefficient as given in Liou (2002) for cirrus size distributions characterized by the effective ice crystal sizes of 10 μm and 42 μm , and the range in the AERONET retrieved AOD 3-hour time series. The radar defined COD values were lower than both the retrieved and the MODIS values for the S13 case, indicating that the satellite retrievals may have been influenced by the strong ocean glint. In the other two cases, the radar defined COD compared very well with the retrievals. In the S22 and O4 cases, the MODIS COD was far in excess of the COD retrievals made by the scheme presented here and that calculated with ground data. In each case, the retrieved AOD mean compared well with the AERONET values even in the strong sun glint case of S13, despite the fact that only 10% of the scene was retrievable.

Figure 2 shows the reflectance in the 0.65 μm and 1.38 μm bands as well as the retrieved AOD and COD

of the O4 case. It can be seen from the 1.38 μm reflectance that cirrus existed throughout the scene in varying degrees. Low cloud is also apparent with high visible and low 1.38 μm reflectance values in the top-middle and as a line to the west of the island. Areas of low cloud and those of thick cirrus will appear black on the subsequent AOD and COD plots since no retrievals were performed. AOD was able to be retrieved elsewhere with a range of values from 0.12 to 0.29 in good comparison with the AERONET range. The retrieved COD standard deviation was large at 0.42 due to the presence of both very visible thin and thick cloud.

4. CONCLUSION

We have developed a method to estimate both the aerosol and thin cirrus contributions to the total atmospheric optical depth occurring in a single satellite field-of-view. This method is based on the principal of radiative transfer and employs a parameterization of the atmospheric reflectance so that the contributions from cirrus, aerosol, and the surface can be separated. In this development, we require an accurate estimate of the surface reflectance as well as the precise removal of reflectance due to cirrus clouds. This is accomplished through careful interpretation of nearby clear sky data and through an empirical method which correlates cirrus reflectance in the 1.38 μm band to that of the visible and near-infrared non-absorbing channels. The retrieved optical depths for aerosols and thin cirrus compare well to ground-based measurements from the Nauru TWP-ARM site. Cirrus retrievals were validated using theoretical cloud extinction values and radar cloud thickness data. Aerosol retrievals were verified by ground-based AERONET data. We demonstrate that this procedure has the potential to increase the area where retrievals of aerosol optical depth can be made over the ocean.

ACKNOWLEDGMENTS

We would like to acknowledge Dr. Brent Holben from the NASA Goddard Space Flight Center for the AERONET data, and Dr. Gerald Mace at the University of Utah for the mm-wave radar data. MODIS data was obtained from the NASA GES DAAC center. This research was supported by DOE grant DE-FG03-00ER62904, JPL/NASA grant 1241575, and AFOSR grant F49620-01-1-0057.

REFERENCES

- Ackerman, S. A., K. I. Strabala, W. P. Menzel, R. Frey, C. Moeller, L. Gumley, B. A. Baum, S. W. Seaman, and H. Zhang, Discriminating clear-sky from cloud with MODIS algorithm theoretical basis document (MOD35), in *ATBD-MOD-06, Version 4.0*, 115 pp., 2002.
- D'Almeida, G., P. Koepke, and E. Shettle, *Atmospheric aerosols: Global climatology and radiative characteristics*, 561 pp., A. Deepak, Hampton, VA, 1991.

- Dessler, A. E. and P. Yang, The distribution of Tropical thin cirrus clouds inferred from Terra MODIS data, *J. Climate*, **16**, 1241-1247, 2003.
- Gao, B. C. and Y. Kaufman, Selection of the 1.375- μm MODIS channel for remote sensing of cirrus clouds and stratospheric aerosols from space, *J. Atmos. Sci.*, **52**, 4231-4237, 1995.
- Heymsfield A. J. and C. M. R. Platt, A parameterization of the particle size spectrum of ice clouds in terms of the ambient temperature and the ice water content, *J. Atmos. Sci.*, **41**, 846-855, 1984.
- King, M. D., S-C Tsay, S. E. Platnick, M. Wang, and K. N. Liou, Cloud retrieval algorithms for MODIS: optical thickness, effective particle radius, and thermodynamic phase (MOD06), in *ATBD-MOD-05*, 79 pp., 1997.
- Liou, K. N., *An Introduction to Atmospheric Radiation*, 2nd Ed., 583 pp., Academic press, San Diego, CA, 2002.
- Martins, J. V., D. Tanre, L. Remer, Y. Kaufman, S. Mattoo, and R. Levy, MODIS cloud screening for remote sensing of aerosols over oceans using spatial variability, *Geophys. Res. Lett.*, **29**, MOD 4, 2002.
- Mishchenko, M. I., I. V. Geogdzhayev, B. Cairns, W. B. Rossow, and A. A. Lacis, Aerosol retrievals over the ocean by use of channels 1 and 2 AVHRR data: sensitivity analysis and preliminary results, *Appl. Opt.*, **38**, 7325-7341, 1999.
- Rolland, P., K. N. Liou, M. D. King, S. C. Tsay, and G. M. McFarquhar, Remote sensing of optical and microphysical properties of cirrus clouds using Moderate-Resolution Imaging Spectroradiometer channels: Methodology and sensitivity to physical assumptions, *J. Geophys. Res.*, **105**, 11,721-11,738, 2000.
- Roskovensky, J. K. and K. N. Liou, Detection of thin cirrus from 1.38 μm /0.65 μm reflectance ratio combined with 8.6 - 11 μm brightness temperature difference, *Geophys. Res. Lett.*, **30**, doi:10.1029/2003GL018135, 2003.
- Takano, Y. and K. N. Liou, Solar radiative transfer in cirrus clouds. Part I: Single-scattering and optical properties of hexagonal ice crystals; Part II: Theory and computation of multiple scattering in an anisotropic medium, *J. Atmos. Sci.*, **46**, 3-36, 1989.
- Wylie, D. P. and W. P. Menzel, Eight years of global high cloud statistics using HIRS. *J. Climate*, **12**, 170-184, 1999.

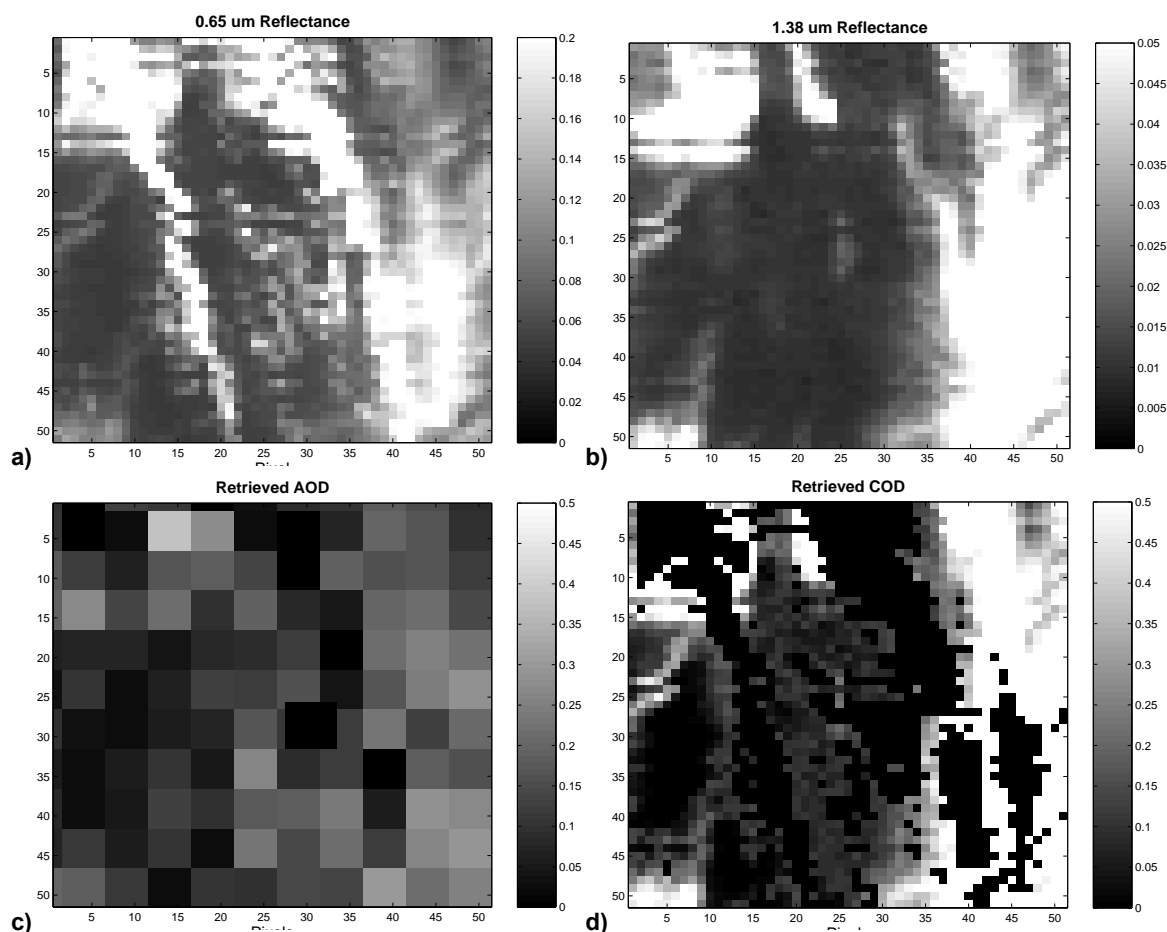


Figure 2. The (a) 0.65 μm reflectance, (b) 1.38 μm reflectance, (c) retrieved AOD, and (d) retrieved COD from the 51 x 51 pixel region centered over the Republic of Nauru on October 4, 2001 (2350 UTC).